

Double-Q spin-density wave in iron arsenide superconductors

J. M. Allred,^{1,*} K. M. Taddei,^{1,2} D. E. Bugaris,¹ M. J. Krogstad,^{1,2} S. H. Lapidus,³ D. Y. Chung,¹ H. Claus,¹ M. G. Kanatzidis,^{1,4} D. E. Brown,² J. Kang,⁵ R. M. Fernandes,⁵ I. Eremin,⁶ S. Rosenkranz,¹ O. Chmaissem,^{1,2} and R. Osborn¹

¹Materials Science Division, Argonne National Laboratory, Argonne, IL 60439-4845, USA

²Physics Department, Northern Illinois University, DeKalb, IL 60115, USA

³Advanced Photon Source, Argonne National Laboratory, Argonne, IL 60439-4845, USA

⁴Department of Chemistry, Northwestern University, Evanston, IL 60208-3113, USA

⁵School of Physics and Astronomy, University of Minnesota, Minneapolis, MN 55455, USA

⁶Institut für Theoretische Physik III, Ruhr-Universität Bochum, 44801 Bochum, Germany

(Date: April 20, 2018)

Elucidating the nature of the magnetic ground state of iron-based superconductors is of paramount importance in unveiling the mechanism behind their high temperature superconductivity. Until recently, it was thought that superconductivity emerges only from an orthorhombic antiferromagnetic spin phase, which can in principle be described in terms of either localized or itinerant spins. However, we recently reported a tetragonal spin structure inside the magnetically ordered state of a hole-doped BaFe_2As_2 . This observation is interpreted as indirect evidence of a new double-Q magnetic state, but alternative models of orbital order could not be ruled out. Here, we present neutron diffraction data that show unambiguously that half of the iron sites in this tetragonal phase are non-magnetic, establishing conclusively the existence of a novel magnetic ground state in a non-nifom magnetization state in contrast to the localized spin We have that this state is naturally explained as the interference between q -spin densities demonstrating the itinerant character of the magnetism of these materials and the invariable presence of magnetic order orbital degrees of freedom.

PACS numbers: 74.70.Xa, 74.25.Ha

INTRODUCTION

One of the central questions to be answered in the iron-based superconductors is the nature of their magnetic interactions. Because superconductivity occurs in proximity to a magnetic instability, it is believed that magnetic fluctuations play a key role in promoting superconducting order [1, 2]. In these materials, the iron atoms in each plane sit on a square lattice and the antiferromagnetic state, from which superconductivity emerges, usually consists of stripes of iron spins aligned ferromagnetically along one iron-iron bond direction and antiferromagnetically along the the other, with a two-fold symmetry that breaks the four-fold symmetry of the high temperature phase. Different theoretical approaches have been proposed to describe the origin of this magnetic two-fold (C_2) state, as well as the associated “nematic” state, and its relationship to superconductivity [3–6].

On the one hand, the large resistivities and enhanced effective masses of the iron arsenides and chalcogenides have been interpreted as evidence for proximity to a Mott transition, as seen in the similar phase diagrams of cuprate superconductors [7–9]. This favours an approach based on localized spin models, in which the iron spins \mathbf{S}_i , with fixed amplitude M , live on the sites i of the iron lattice and interact with each other *via* exchange interactions. This can give rise to superconductivity with extended s -wave symmetry, in which the order parameter changes sign between next-nearest neighbor sites. Some

localized models focus not on magnetic, but on orbital degrees of freedom, whose fluctuations in general favour a regular s -wave state [10, 11]. In this case, magnetic order is a secondary effect of the four-fold symmetry breaking produced by changing the relative occupation of the d_{xz} and d_{yz} iron orbitals.

On the other hand, itinerant spin models rely on the metallic character of these compounds and on quasi-nesting features of their Fermi surfaces [12, 13]. In this case, instead of local spins on the lattice sites, the magnetism is best described as a modulation of the spin polarization of the itinerant electrons, *i.e.*, a spin-density wave, $\mathbf{S}(\mathbf{r}) = \mathbf{M} \cos(\mathbf{Q} \cdot \mathbf{r})$, with $\mathbf{Q} = (\pi, 0)$ or $(0, \pi)$. The resulting superconducting symmetry depends on details of the Fermi surface, and is usually extended s -wave but can also be d -wave. Determining which approach is valid, itinerant or localized, will therefore have profound consequences both for the nature of the emergent superconductivity and its relation to cuprate superconductivity [6].

Because both the localized and itinerant scenarios predict ground states with the same space group, distinguishing between them is a challenging task. Recently, we observed a new magnetic phase in hole-doped BaFe_2As_2 that offers a new way to resolve this issue [14]. In pure BaFe_2As_2 , the structural, orbital and magnetic transitions occur simultaneously in a first-order transition. When sodium is doped onto the barium sites, the transition temperature, T_N , is reduced until magnetic or-

der is destroyed at $x \lesssim 0.3$ [15]. However, between $0.24 \lesssim x \lesssim 0.3$, four-fold (C_4) symmetry is restored inside the magnetically ordered state at T_r ($T_r < T_N$), with a reorientation of the magnetic moments along the c -axis [16]. Because the magnetic Bragg peaks have the same reciprocal lattice indices above and below T_r , this C_4 phase was interpreted as a double- \mathbf{Q} magnetic structure described by a coherent superposition of two spin-density waves, $\mathbf{S}(\mathbf{r}) = \mathbf{M}_1 \cos(\mathbf{Q}_1 \cdot \mathbf{r}) + \mathbf{M}_2 \cos(\mathbf{Q}_2 \cdot \mathbf{r})$, with $\mathbf{Q}_1 = (\pi, 0)$ and $\mathbf{Q}_2 = (0, \pi)$.

Although such order is naturally predicted by itinerant models for the iron-based superconductors [14, 17–20], it was not possible to rule out the existence of an orbitally ordered structure that is consistent with the observed C_4 phase. Furthermore, the existence of magnetic Bragg peaks at both \mathbf{Q}_1 and \mathbf{Q}_2 could be ascribed to domains of stripe magnetic order instead of double- \mathbf{Q} order. Khalyavin *et al.* discuss a number of orbitally ordered structures that are compatible with the diffraction [21]. Common to all of them is that the crystal structure is tetragonal, but the magnetic structure still consists of orthorhombic (*i.e.*, single- \mathbf{Q}) stripes.

In this paper, we present unambiguous evidence that the magnetic state of a hole-doped iron arsenide, $\text{Sr}_{1-x}\text{Na}_x\text{Fe}_2\text{As}_2$ with $x = 0.37$, is a double- \mathbf{Q} spin-density wave. This is the third hole-doped compound within the $A\text{Fe}_2\text{As}_2$ series ($A = \text{Ba}, \text{Sr}$) to show signatures of the C_4 phase, indicating that this is a universal feature of hole-doping [14, 22, 23]. We were able to synthesize powders that exhibit a complete transformation of the sample to the C_4 phase below T_r , allowing us to utilize Mössbauer spectroscopy as a local probe of the magnetization on the ^{57}Fe sites. Below T_N , within the C_2 phase, all sites show the same Zeeman splitting due to internal molecular fields as expected for the single- \mathbf{Q} stripes. However, below the C_4 transition at $T_r < T_N$, 50% of the iron sites are non-magnetic while the other 50% show a doubling of the magnetization, exactly as expected from a double- \mathbf{Q} structure formed by the interference between two collinear spin-density waves, $\mathbf{S}(\mathbf{r}) = \mathbf{M}_1 \cos(\mathbf{Q}_1 \cdot \mathbf{r}) + \mathbf{M}_2 \cos(\mathbf{Q}_2 \cdot \mathbf{r})$, with $\mathbf{M}_1 = \mathbf{M}_2$. This redistribution of magnetization density is not compatible with the idea of local moments living on the iron sites or with any form of orbital order. Therefore, our results point to the primary role played by itinerant magnetism in the phase diagram of the iron arsenides, offering a key insight into the nature of the electronic state from which superconductivity emerges.

RESULTS

X-ray and Neutron Diffraction

Magnetism in the hole-doped series, $\text{Sr}_{1-x}\text{Na}_x\text{Fe}_2\text{As}_2$, has higher transition temperatures and persists to higher

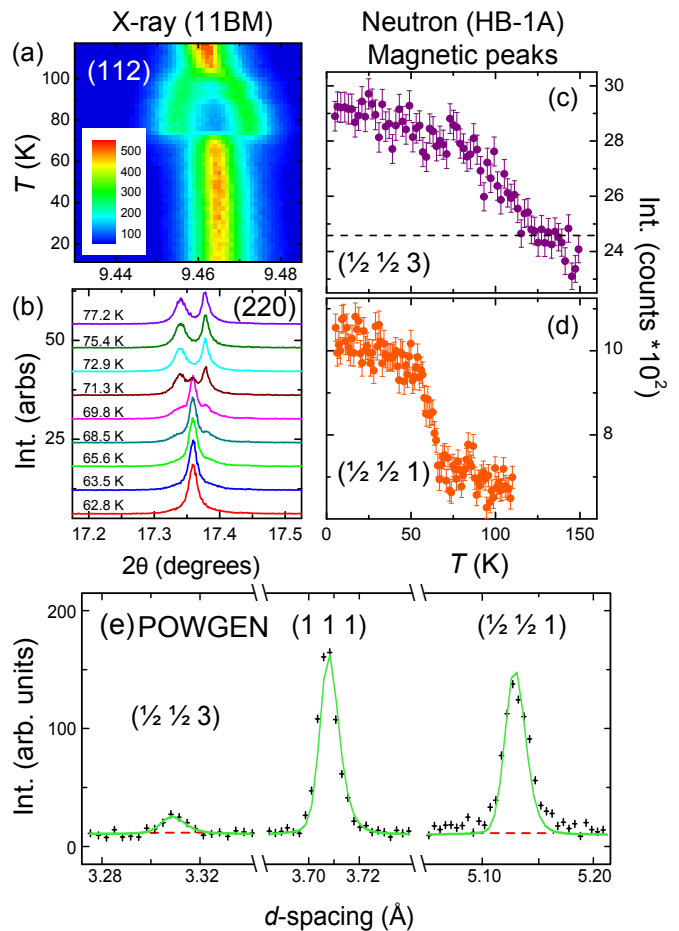


FIG. 1. Temperature dependent diffraction data of $\text{Sr}_{0.63}\text{Na}_{0.37}\text{Fe}_2\text{As}_2$. Left panels (a-b) are from x-ray (11BM, $\lambda = 0.413842 \text{ \AA}$) and the right panels (c-d) are from constant wavelength neutrons (HB-1A, $\lambda = 2.3626 \text{ \AA}$). (a) is a false color map of the data and the tetragonal (112) peak, and (b) is a view of the tetragonal (220) peak at temperatures near T_r taken from the same data. (c) and (d) show the intensity of the $(\frac{1}{2} \frac{1}{2} 3)$ and $(\frac{1}{2} \frac{1}{2} 1)$ magnetic peaks, respectively. (e) Detailed view of the calculated intensity (green line) from the magnetic model fit to the 10 K POWGEN data (black crosses). The dotted red line shows the calculated intensities of a non-magnetic model.

levels of sodium concentration than the equivalent barium series [15, 24]. We synthesized a compound with the nominal composition of $\text{Sr}_{0.63}\text{Na}_{0.37}\text{Fe}_2\text{As}_2$, below the critical phase boundary for magnetic order, which has a superconducting transition at 12 K. Rietveld refinements of the x-ray powder diffraction spectra yielded a sodium concentration of $x = 0.3691(5)$. More details of the sample characterization are provided in the Methods section and the Supplementary Information.

The transition from tetragonal ($I4/mmm$) to orthorhombic ($Fmmm$) symmetry is evident in the powder x-ray diffraction as a splitting of some of the Bragg peaks, such as the (112) peak, shown in Figure 1a. This C_2 transition, which is either weakly first order or second

order, occurs around $T_N \approx 105(2)$ K, below which the orthorhombic order parameter (*i.e.*, the magnitude of peak splitting) increases rapidly with decreasing temperature. This behaviour is similar to many other iron-based superconductors, but more unusually, this sample then transforms back to tetragonal symmetry at a strongly first order transition at $T_r \approx 73$ K. The first-order nature of this transition from C_2 to C_4 symmetry can be seen in Figure 1b, which shows that the two phases coexist for ~ 10 K below T_r .

Powder neutron diffraction confirms that both the C_2 and C_4 phases are magnetically ordered. Both the $(\frac{1}{2} \frac{1}{2} 1)$ and $(\frac{1}{2} \frac{1}{2} 3)$ magnetic peaks are present below T_N (Figure 1c and d), but the increase in intensity of the former at T_r shows that there is a significant spin reorientation in the C_4 phase, as observed in $\text{Ba}_{1-x}\text{Na}_x\text{Fe}_2\text{As}_2$ ($0.24 \leq x \leq 0.28$) [14]. Since the transformation back to tetragonal symmetry is complete in $\text{Sr}_{0.63}\text{Na}_{0.37}\text{Fe}_2\text{As}_2$ below 60 K, we are able to obtain a more reliable refinement of the magnetic structure than was possible in the earlier work. Figure 1e shows that the data are fit well by a model with moments along c -axis, in agreement with the moment direction deduced by Waßer *et al.* [16].

The magnetic Bragg peaks in the C_4 phase have the same reciprocal lattice indices as the C_2 phase, using the tetragonal unit cell, so one possible interpretation of the data is that the two phases have identical magnetic stripe order, only differing by the orientation of the iron spins. In this single- \mathbf{Q} model, Bragg peaks from stripes parallel to the x and y axes in different domains would be incoherently superposed (Fig. 2a). Such a model would be magnetically orthorhombic, so magnetoelastic coupling should generate an orthorhombic structural distortion as well, but it is plausible that it is much weaker because of the spin reorientation and therefore difficult to resolve.

An alternative interpretation is that there is a single domain comprising a coherent superposition of magnetic stripes parallel to both the x and y axes, a double- \mathbf{Q} model (Fig. 2b). This is the model predicted by itinerant approaches, in which magnetic order in the C_4 phase is generated by band nesting along the x and y directions simultaneously, restoring tetragonal symmetry [14]. In such a case, the residual spin-orbit coupling allows the parallel orientation of the resulting magnetic moments from each wave vector only if they are along the z -direction. It is well known that diffraction alone is unable to distinguish between multi-domain single- \mathbf{Q} and single-domain multi- \mathbf{Q} structures, since they produce identical Bragg peak intensities. As discussed in Ref. 21, it might be possible to distinguish them with resonant x-ray scattering, which is sensitive to the orbital configuration of the iron d -electrons. In particular, space groups compatible with any possible orbital order would be incompatible with a double- \mathbf{Q} model.

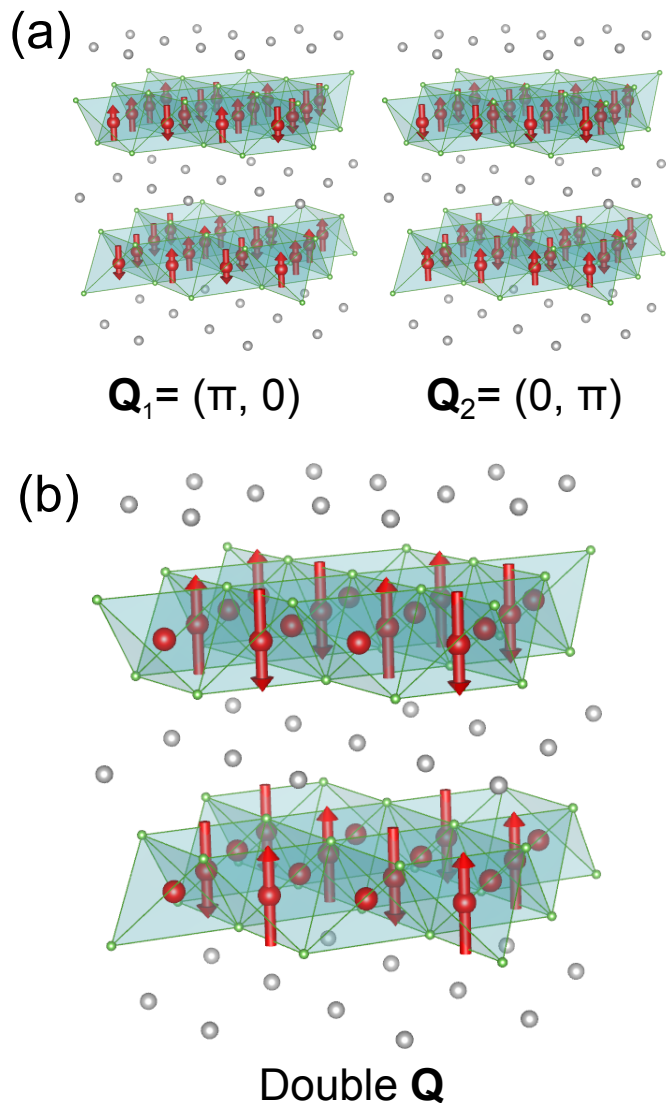


FIG. 2. Single- \mathbf{Q} and double- \mathbf{Q} magnetic models (a) Single- \mathbf{Q} model, in which spins are modulated in either $\mathbf{Q}_1 = (\pi, 0)$ or $\mathbf{Q}_2 = (0, \pi)$, parallel to the a and b axes respectively in different domains (b) Double- \mathbf{Q} model, formed from the superposition of modulations along \mathbf{Q}_1 and \mathbf{Q}_2 .

Mössbauer Spectroscopy

Although in reciprocal space, the single- \mathbf{Q} and double- \mathbf{Q} models look identical, they are remarkably different in real space. As shown in Figure 2b, the coherent superposition of the orthogonal stripes in the double- \mathbf{Q} model results in a doubling of the magnetic moments on half of the sites and a complete cancellation of the magnetic moments on the other half. That is, half of the iron sites are spin-density wave nodes. In local moment systems, nodes represent fluctuating spins that have a high entropy, but in an itinerant spin-density wave, they can be a natural consequence of a spatially inhomogeneous magnetization.

The best way to distinguish these two magnetic struc-

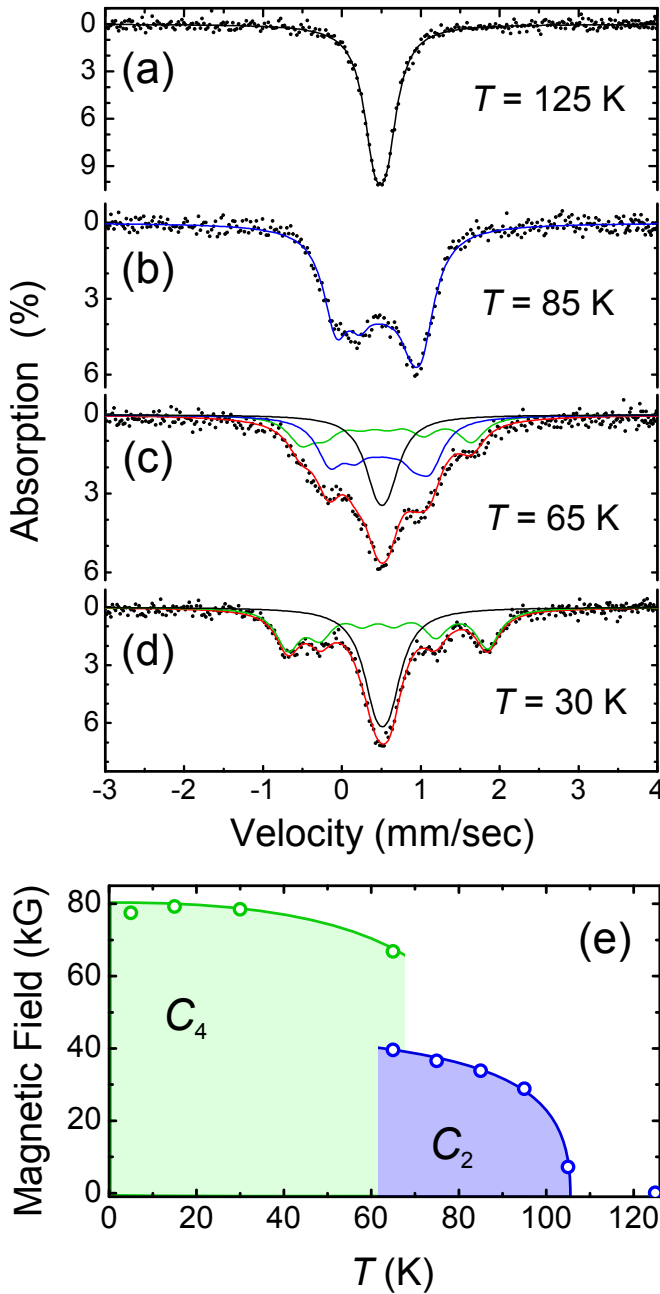


FIG. 3. (a-d) Mössbauer spectra (black circles) at 30, 65, 85, and 125 K (5, 15, 75, 95, and 105 K not shown). First the conditions of differentiation are non-magnetic sites (black lines), C_4 magnetic sites (green lines), C_2 magnetic sites (blue lines) and paramagnetic (red lines). (e) Effective magnetic field on each magnetic site as a function of temperature determined from Mössbauer spectroscopy. The lines are guides to the eye. Error bars are smaller than the pins.

tures is therefore to use a local probe of the magnetization. Mössbauer spectroscopy is ideal because the Zeeman splitting of the nuclear levels of ^{57}Fe atoms is directly proportional to the static magnetization density at the nuclear site. Earlier Mössbauer spectra on iron

arsenides were consistent with the temperature dependence of the conventional antiferromagnetic stripe order, which is characterized by a single hyperfine field at each temperature [25, 26].

We have measured Mössbauer spectra at temperatures between 5 K and 125 K (Figure 3). The 125 K spectrum shows, as expected, a single peak associated with the paramagnetic phase, with a small isomer shift due to the chemical environment that is independent of temperature. Spectra measured in the C_2 phase at 95, 85 and 75 K (only 85 K is shown) are well fit with a single hyperfine field, characteristic of a single magnetic site, which grows with decreasing temperature (Figure 3e). However, well below the C_4 transition, at 30 K, there is a qualitatively different spectrum, which consists of a large central peak with the same isomer shift as the paramagnetic phase, indicating the presence of non-magnetic sites, and a sextet indicating magnetic sites with a significantly larger effective field than in the C_2 phase (by a factor of ~ 2). A free fit to such a two-site model shows that the spectral weights of each component are identical within the statistical uncertainty. In other words, 50% of the sites are magnetic and 50% are non-magnetic, exactly as predicted by the double- \mathbf{Q} model.

The 65 K spectrum, which was taken in the temperature range where diffraction data indicated a co-existence of the C_4 and C_2 phases, shows evidence of the superposition of three components, two magnetic and one non-magnetic. Although the parameters are too highly correlated to be fit independently, the spectrum is consistent with a C_4 contribution, comprising an equal concentration of large moment and non-magnetic sites, and a C_2 contribution from smaller moment sites. Another parameter, the electric field gradient, which is sensitive to the point-group symmetry of the surrounding ions, changes sign between the C_2 and C_4 phases, but is otherwise nearly temperature independent. The resulting local magnetization of the magnetic sites as a function of temperature (Figure 3e) shows a clear doubling of the magnetic moment within the C_4 phase compared to the C_2 phase, demonstrating that the C_4 magnetic structure involves a redistribution of magnetization density from the non-magnetic to the magnetic sites, an effect that is a clear fingerprint of an itinerant spin density wave.

DISCUSSION AND CONCLUSION

The Mössbauer data provide unambiguous evidence that the magnetism in the C_4 phase is a double- \mathbf{Q} spin-density wave. This has a number of important consequences. As pointed out in Ref. 21, such a double- \mathbf{Q} magnetic structure is incompatible with either ferro-orbital order involving the d_{xz} and d_{yz} iron orbitals or with more complex patterns of orbital ordering. As a result, it implies that the nematic phase observed in the

underdoped compounds is not the cause, but a consequence of magnetism, in agreement with the spin-nematic scenario [27]. Although this observation by itself cannot rule out the existence of orbital fluctuations, which favour the more conventional *s*-wave superconducting state, it does indicate the primary role played by magnetic fluctuations, which favour the unconventional sign-changing extended *s*-wave state.

The most important conclusion to be drawn from this work is that the nature of the C_4 magnetic state is not consistent with a model of localized spins on the iron sites, in which every iron site is magnetic. At least within the t - J_1 - J_2 model, widely employed as an effective model to study these materials [8, 28, 29], such a non-uniform magnetization is not a ground state of the model. It remains to be seen whether modifications of this model, such as the inclusion of non-Heisenberg exchange interactions, like the biquadratic or ring exchanges, could describe the non-uniform state.

By contrast, an itinerant approach offers a natural explanation of this non-uniform magnetic structure as the interference of two nesting-related spin density waves, $\mathbf{S}(\mathbf{r}) = \mathbf{M}_1 \cos(\mathbf{Q}_1 \cdot \mathbf{r}) + \mathbf{M}_2 \cos(\mathbf{Q}_2 \cdot \mathbf{r})$, with \mathbf{M}_1 and \mathbf{M}_2 parallel to each other. The fact that $M_1 = M_2$ ensures not only the tetragonal symmetry of the system, in agreement with the experimental observations, but also implies that half of the sites are non-magnetic with their spin density transferred to neighbouring sites with double the magnetization. This is a remarkable observation that is only compatible with itinerant electrons. It is also consistent with the prediction of itinerant models that such a state becomes favoured over the stripe state for large enough doping levels [14, 17, 19, 20, 30]. Furthermore, a secondary checkerboard charge order should accompany this non-uniform phase, in which the non-magnetic sites have locally a different charge density than the magnetic sites [31]. It has been argued that fluctuations of this secondary charge order can enhance the extended *s*-wave transition temperature [31].

The reorientation of the magnetization along the *c*-axis follows from general group-theory arguments related to the space-group of a single FeAs plane with preserved tetragonal symmetry [32]. In the iron pnictides, spin-orbit coupling is not small [33], and as a consequence, possible spin orientations are restricted to certain crystallographic directions. In particular, a group-theory analysis reveals three possibilities: $\mathbf{M}_1 \parallel \hat{\mathbf{x}}$ and $\mathbf{M}_2 \parallel \hat{\mathbf{y}}$; $\mathbf{M}_1 \parallel \hat{\mathbf{y}}$ and $\mathbf{M}_2 \parallel \hat{\mathbf{x}}$; or $\mathbf{M}_1 \parallel \hat{\mathbf{z}}$ and $\mathbf{M}_2 \parallel \hat{\mathbf{z}}$. Because only the latter is compatible with the non-uniform state discussed here, the spins must point along the *c*-axis. This is discussed in more detail in the Supplementary Information.

We note that the itinerancy of the magnetism of the iron pnictides does not imply that interactions are necessarily weak [34–36]. Indeed, even in elemental iron, a weak-coupling approach does not fully describe the prop-

erties of the ferromagnetic state. In the iron pnictides, interaction effects were shown to be important to capture high-energy properties of the spin spectrum [37] and the sizable fluctuating moment observed in the paramagnetic state [38]. Thus, it is likely that interactions are moderate, and may affect distinct families of iron-based superconductors, such as the iron chalcogenides, differently [3, 4]. At least in the iron pnictides, however, our work demonstrates that itinerancy is an essential ingredient of these fascinating materials.

METHODS

Synthesis

Handling of all starting materials was performed in an M-Braun glovebox under an inert Ar atmosphere (< 0.1 ppm of H_2O and O_2). Sr (Aldrich, 99.9%) and Fe (Alfa Aesar, 99.99+%) were used as received. Small pieces of Na free of oxide coating were trimmed from large lumps (Aldrich, 99%). Granules of As (Alfa Aesar, 99.99999+%) were ground to a coarse powder prior to use. The precursor materials SrAs, NaAs, and Fe_2As were synthesized in quartz tubes from stoichiometric reactions of the elements at 800°C, 350°C, and 700°C respectively. Polycrystalline samples of $\text{Sr}_{0.67}\text{Na}_{0.37}\text{Fe}_2\text{As}_2$ were prepared from stoichiometric mixtures of SrAs, NaAs, and Fe_2As , which were ground thoroughly with a mortar and pestle, and loaded in alumina crucibles. The alumina crucibles were sealed in Nb tubes under Ar, which were further sealed in quartz tubes under vacuum. The reaction mixtures were subjected to multiple heating cycles between 850–950°C for durations less than 48 h (to minimize loss of Na by volatilization). The samples underwent grinding by mortar and pestle between heating cycles in order to homogenize the compositions. Following the final heating cycles, the sealed samples were quenched in air from the maximum temperature rather than allowing them to cool slowly. Initial characterization of the dark gray powders was conducted by laboratory powder X-ray diffraction and magnetization measurements. More details of the sample characterization are provided in the Supplementary Information.

Powder Diffraction

X-ray powder diffraction measurements were performed at Argonne National Laboratory using beamline 11-BM at the Advanced Photon Source. Neutron powder diffraction measurements were performed at Oak Ridge National Laboratory using beamline HB-1A at the High Flux Isotope Reactor and the POWGEN diffractometer at the Spallation Neutron Source.

Mössbauer Spectroscopy

Mössbauer measurements were performed in transmission geometry with a sinusoidally driven 2 mCi $^{57}\text{Co}(\text{Rh})$ source and a germanium detector. Silicon diode sensors allowed the control and stabilization of the sample temperature to within 0.2 K for a conventional bath cryostat. Powder samples having an effective area density of 4 mg/cm^2 of ^{57}Fe were placed on 99.999% pure aluminum foil held in place by kapton tape. Calibrations were made using a natural $\alpha\text{-Fe}$ foil. The spectra were fit by varying the isomer shift, magnetic hyperfine field, and the electric quadrupole factor. The intensities of the magnetic sextet-split lines were constrained to a 1:2:3 ratio according to their Clebsch-Gordon coefficients (or magnetic dipole matrix elements), and the Lorentzian linewidths for all lines of a particular iron site were constrained to be the same. Details of the fit parameters are given in the Supplementary Information.

* jalled@anl.gov

- [1] Chhkoy A. Pairing mechanism in fe-based ~~pr~~condob *Ann. Rev. Cond. Matt. Phys.* **3**, 5792 (2012).
- [2] Hishfeld, P., Kohnoy M. & Main, I. Gappmety and sta of fe-based ~~pr~~condob *Rep. Prog. Phys.* **74**, 124508 (2011).
- [3] Dai, P., Hu J. & Dagob, E. Magnetsm and ismicosoje oigin in ion-based high-tempona ~~pr~~condob *Nature Phys.* **8**, 709718 (2012).
- [4] Yin, Z. P., Hale, K. & Koliar G. Kinetic faton and he nat of he magnetic and pamagnetic ses in ion picides and ion chalcogenides *Nature Mater.* **10**, 932935 (2011).
- [5] Yu R., Gosmi, P., Si, Q., Nikolic, P. & Zhu J.-X. Sprondotiyathe borderof electron localizaton and imeancy *Nature Comm.* **4**, 2783 (2013).
- [6] Fenandes R. M., Chhkoy A. V. & Schmalian, J. Whatdisnemaic oderin ion-based ~~pr~~condob *Nature Phys.* **10**, 97404 (2014).
- [7] Si, Q. & Abahams E. Song correlatons and magneic faton in he high T_c ion picides *Phys. Rev. Lett.* **101**, 076401 (2008).
- [8] Seo, K., Beneig, B. A. & Hu J. Pairing smmetyin a ~~o~~-obital exchange coling model of opicides *Phys. Rev. Lett.* **101**, 206404 (2008).
- [9] de' Medici, L., Gioannet, G. & Capne, M. Selectiv motpysasa keyo ion ~~pr~~condob *Phys. Rev. Lett.* **112**, 177001 (2014).
- [10] Iger F., Kmar S., Zaanen, J. & an den Bink, J. Spin-obital fatons and anomalosmetallic se in ion-picide ~~pr~~condob *Phys. Rev. B* **79**, 054504 (2009).
- [11] Konani, H., Inou, Y., Saito, T., Yamakas, Y. & Onai, S. Obital faton heoyin ion-based ~~pr~~condob s $^{++}$ -se ~~pr~~condotiyta aniston, and imjinduced nemaic oder *Sol. Stat. Comm.* **152**, 718727 (2012).
- [12] Chhkoy A. V., Efemoy D. V. & Eemin, I. Magneism, sprondotiy and ping smmetyin ion-based ~~pr~~condob *Phys. Rev. B* **78**, 134512 (2008).
- [13] Fenandes R. M. *et al.* Unconventional ping in he ion asnide ~~pr~~condob *Phys. Rev. B* **81**, 140501 (2010).
- [14] Aoi, S. *et al.* Magneticallydiven pion of nemaic oderin an ion-based ~~pr~~condob *Nature Comm.* **5**, 3845 (2014).
- [15] Aoi, S. *et al.* Stal, magneic, and ~~pr~~condotiyng ppies of Ba $_{1-x}\text{Na}_x\text{Fe}_2\text{As}_2$. *Phys. Rev. B* **88**, 094510 (2013).
- [16] Wafer F. *et al.* Spin eorientaton in Ba $_{0.65}\text{Na}_{0.35}\text{Fe}_2\text{As}_2$ dlied by angle-chl netin diffraction. *Phys. Rev. B* **91**, 060505 (2015).
- [17] Gioannet, G. *et al.* Poimiof ion picide ~~pr~~condob a qm icritical pint *Nature Comm.* **2**, 398 (2011).
- [18] Eemin, I. & Chhkoy A. V. Magnetic degeneacy and hidden metallicity of he ~~pr~~-denitow se in fer opicides *Phys. Rev. B* **81**, 024511 (2010).
- [19] Bylon, P. M. R., Schmiedt J. & Timm, C. Microsoje callydeivd ginby-landaheoyformagnetic oder in he ion picides *Phys. Rev. B* **84**, 214510 (2011).
- [20] Wang, X., Kang, J. & Fenandes R. M. Magnetic oder in otthagonal-smmetybreaking in ion asnides Microsoje mechanism and ~~pr~~-se pctn. *Phys. Rev. B* **91**, 024401 (2015).
- [21] Khalayn, D. D. *et al.* Symmety of eenantaggonal has in Ba $_{1-x}\text{Na}_x\text{Fe}_2\text{As}_2$: Magnetic ~~o~~obital odering mechanism. *Phys. Rev. B* **90**, 174511 (2014).
- [22] Blimer A. E. *et al.* Sprondotiyinduced eenance of oohombic diston in Ba $_{1-x}\text{K}_x\text{Fe}_2\text{As}_2$. *arXiv* 1412.70382 (2014).
- [23] Alled, J. M. *et al.* Tetagonal magnetic has in Ba $_{1-x}\text{K}_x\text{Fe}_2\text{As}_2$ fom ~~xy~~ and netin diffraction. *arXiv* 1505.014334 (2015).
- [24] Cots Gil, R. & Clake, S. J. Stal, Magnetsm, and Sprondotiy of he Layered Ion Asnides $\text{Sr}_{1-x}\text{Na}_x\text{Fe}_2\text{As}_2$. *Chem. Mater.* **23**, 10094016 (2011).
- [25] McGie, M. *et al.* Phas anistons in LaFeAsO: Stal, magneic, elak, and anppropies heat capcity and Msaeer pct. *Phys. Rev. B* **78**, 094517 (2008).
- [26] Kito, S. *et al.* Spin Odering in LaFeAsO and Its Sp pion in Sprondob LaFeAsO 0.89F 0.11P obed by Msaeer Spctosop *J. Phys. Soc. Japan* **77**, 103706 (2008).
- [27] Fenandes R. M., Chhkoy A. V., Knolle, J., Eemin, I. & Schmalian, J. Pemptv nemaic oder ~~pd~~ogap and obital oderin he ion picides *Phys. Rev. B* **85**, 024534 (2012).
- [28] Ly W., Wu J. & Phillip P. Obital odering induces stal has aniston and he ~~o~~ssyanomalyin ion picides *Phys. Rev. B* **80**, 224506 (2009).
- [29] Yu R., Zhu J.-X. & Si, Q. Obital-selectiv ~~pr~~condotiygapanistob and ~~pr~~esonance excitatons in a mllobital J_1 - J_2 model for ion picides *Phys. Rev. B* **89**, 024509 (2014).
- [30] Gakaso, M. N. & Andersen, B. M. Comping magnetic doble-Q has and ~~pr~~condotiyinduced eenance of C_2 magnetic ~~sp~~ oderin ion picides *arXiv* 1502.05859 (2015).

- [31] Fernandes R. M., Kienle, S. A. & Beg, E. Is there a hidden chiral density in the iron-based perovskites? *arXiv* 1504.03656 (2015).
- [32] Cokoic, V. & Vafeek, O. Space group symmetry, orbital coupling, and the low-energy effective Hamiltonian for iron-based perovskites *Phys. Rev. B* **88**, 134510 (2013).
- [33] Boisenko, S. *et al.* Direct observation of in-orbital coupling in iron-based perovskites *arXiv* 1409.8669 (2014).
- [34] Johannes M. D. & Mañá, I. I. Microscopic origin of magnetism and magnetic interactions in ferrimagnets *Phys. Rev. B* **79**, 220510 (2009).
- [35] Yin, W.-G., Lee, C.-C. & Kim, W. Unified picture of magnetic correlations in iron-based perovskites *Phys. Rev. Lett.* **105**, 107004 (2010).
- [36] Basoň E., Valenzuela, B. & Caldeón, M. J. Orbital differentiation and the role of orbital ordering in the magnetic state of Fe perovskites *Phys. Rev. B* **86**, 174508 (2012).
- [37] Yin, Z., Hale, K. & Kotlar, G. Magnetism and charge dynamics in iron perovskites *Nature Phys.* **7**, 294297 (2011).
- [38] Hansmann, P. *et al.* Dichotomy between large local and small ordered magnetic moments in iron-based perovskites *Phys. Rev. Lett.* **104**, 197002 (2010).

END NOTES

Acknowledgements

This work was supported by the U.S. Department of Energy, Office of Science, Materials Sciences and Engineering Division and Scientific User Facilities Division.

X-ray experiments were performed at the Advanced Photon Source, which is supported by the Office of Basic Energy Sciences under Contract No. DE-AC02-06CH11357. Neutron experiments were performed at the High Flux Isotope Reactor and Spallation Neutron Source. R.M.F. and J.K. were supported by the U.S. Department of Energy, Office of Science, Basic Energy Sciences, under award number de-sc0012336. The work of I.E. was supported by the Focus Program 1458 Eisen-Pnictide of the DFG, and by the German Academic Exchange Service (DAAD PPP USA no. 57051534). The authors thank A. A. Aczel, A. Huq, M. J. Kirkham, and P. S. Whitfield for experimental assistance, E. E. Alp for use of his Mössbauer spectrometer, and B. M. Andersen, A. V. Chubukov, M. N. Gastiasoro, A. Yaresko, and Y. Zhao for fruitful discussions.

Author contributions

Samples were prepared by D.E.Bu., with additional support from D.Y.C., and M.G.K. The experiments were devised by J.M.A., K.M.T., O.C., S.R., and R.O. The x-ray and neutron diffraction experiments were performed by J.M.A., K.M.T., O.C., M.J.K., S.R., and S.H.L. Mössbauer spectroscopy was performed by D.E.Br. Magnetization measurements were performed by H.C. The data were analyzed by J.M.A., K.M.T., O.C., S.R., R.O., and D.E.Br. Theoretical interpretation was provided by J.K., R.M.F. and I.E. The manuscript and supplementary information were written by J.M.A., R.O., R.M.F., and I.E. with input from all the authors.